Supporting Information

p-block main-group metal-based two-dimensional metal-organic frameworks as efficient electrocatalysts for oxygen reduction reaction

Yanan Zhou,[a] Xiaoping Gao*[b] and Wenhua Zhang*[c]

[a]School of Material Science and Chemical Engineering, Ningbo University, Ningbo, Zhejiang 315211, China.
[b]School of New Energy, Ningbo University of Technology, Ningbo, Zhejiang 315336, China
[c]Department of Materials Science and Engineering, University of Science and Technology of China, Hefei, Anhui 230026, China

*Corresponding author:
Email: whhzhang@ustc.edu.cn
Email: gaoxiaoping2014@foxmail.com.

1. ORR

The cathodic ORR process follows a four-stage pathway to generate H_2O product and the four electron reaction paths are defined as equations (a) - (d) as reported in the previous literature[1]:

$* + O_2\,(g) + H^+ + e^- \rightarrow HOO*$ (a)

$HOO* + H^+ + e^- \rightarrow O* + H_2O\,(l)$ (b)

$O* + H^+ + e^- \rightarrow HO*$ (c)

$HO* + H^+ + e^- \rightarrow H_2O\,(l) + *$ (d)

Where * represents active sites on the catalyst, (*l*) and (g) is the liquid and gas phase, respectively, and HOO*, O* and HO* are the corresponding adsorbed intermediates. The Gibbs free energy (ΔG) of each elementary step under the U = 0 and pH = 0 condition was calculated by the following equations (1a~1d):

$\Delta G_a = G_{HOO*} - G_* - 1/2G_{H2,g} - \{4.92eV + 2G_{H2O,l} - 2G_{H2,g}\}$ (1a)

$$\triangle G_b = G_{H2O,l} + G_{O*} - G_{HOO*} - 1/2G_{H2,g} \quad (1b)$$

$$\triangle G_c = G_{HO*} - G_{O*} - 1/2G_{H2,g} \quad (1c)$$

$$\triangle G_d = G_{H2O,l} + G_{*} - G_{HO*} - 1/2G_{H2,g} \quad (1d)$$

Where we defined $G_{X*}=E_{X*}+ZPE_{X*}-TS_{X*}$, X refers to HOO*, O* and HO*. Here E_{X*} is the DFT total energy of the corresponding X* system under the polarization solvent model calculation. ZPE_{X*} refers to the zero-point energy of X*. Here we only include the zero-point energy of X*, while keeping the catalyst * fixed. TS_{X*} is the calculated entropy term of the adsorbed intermediate. Finally, $G_{*}=E_{*}$ is the total energy of catalyst under the DFT solvent model calculation. Due to the poor description of DFT for the high-spin ground state of the O_2, we used $G_{O2,g} + 4G_{H2,g} - 2G_{H2O,l} = 4.92$ eV to obtain the free energy of O_2 in the gas phase.[2] It is also difficult to directly calculate the Gibbs free energy of H_2O in the liquid phase ($G_{H2O,l}$). It is customary to calculate the liquid phase Gibbs free energy from its vapor phase counterpart at their equilibrium pressure when they have the same Gibbs free energies. Then, $G_{H2O,l} = E_{H2O} + ZPE_{H2O} - TS_{H2O}$. Where, E_{H2O} is total energy of H_2O in the gas phase obtained from the DFT calculation; ZPE_{H2O} is the zero point energy; TS_{H2O} is the entropy term of the gas phase (in equilibrium with the liquid phase). We took the values of 0.67 eV and 0.41 eV for the TS_{H2O} and TS_{H2}, respectively.[3] As the most important measure of the catalytic activities for ORR, overpotential η of ORR (η^{ORR}) was calculated by equation (2):

$$\eta^{ORR} = 1.23 - \frac{\min\{\Delta G_a,\ \Delta G_b,\ \Delta G_c,\ \Delta G_d\}}{e} \quad (2)$$

2. The catalytic selectivity of the ORR

The rate constant *k* can be obtained based on the Arrhenius equation: $k = A \exp(-\Delta G_{PDS}/k_B T)$. Here, *A*, k_B and T refers to the pre-exponential factor, the Boltzmann constant and the temperature of 298.15 K, respectively. Hence, we can obtain the following equation: $\ln(k_{sys}/k_{Pt(111)}) = [\Delta G_{PDS}(Pt(111) - \Delta G_{PDS}(sys)]/k_B T$. Here, k_{sys} and $k_{Pt(111)}$ refer to the rate constant of the ORR on the screened electrocatalysts and ORR on the benchmark catalyst Pt(111), respectively. The selectivity of a certain catalyst can be estimated from the ratio of rate constants k_{O2} and k_{H2O2} as shown in the following equation: $\ln(k_{O2}/k_{H2O2}) = [\Delta G(H_2O_2 - \Delta G(O*)]/k_B T$. Here, k_{O2} and k_{H2O2} refers to the rate constant of O* formation from HOO* and

H_2O_2 formation from HOO*, respectively.

3. The polarization curves simulation of ORR

The ORR polarization curves of PMN_xO_{4-x}-HADQ catalysts were simulated based on the kinetic model developed by Hansen et al.[4] In this work, we focused on the dominating associative mechanism of the ORR. We simplified the above method and considered the corresponding electrochemical reduction steps as shown in the following equations:

$$O_2^* + H^+ + e^- \underset{k_{-1}}{\overset{k_1}{\rightleftarrows}} HOO* \quad \text{(S1)}$$

$$HOO* + H^+ + e^- \underset{k_{-2}}{\overset{k_2}{\rightleftarrows}} O* + H_2O \quad \text{(S2)}$$

$$O* + H^+ + e^- \underset{k_{-3}}{\overset{k_3}{\rightleftarrows}} HO* \quad \text{(S3)}$$

$$HO* + H^+ + e^- \underset{k_{-4}}{\overset{k_4}{\rightleftarrows}} * + H_2O \quad \text{(S4)}$$

Here, k_i and k_{-i} refers to the rate constants of reaction and reverse reaction, respectively. Based on the above reaction steps, the corresponding rate equations of intermediates can be calculated by the following equations:

$$\frac{\partial \theta_{HOO^*}}{\partial t} = -k_2\theta_{HOO^*} + k_{-2}\theta_{O^*}x_{H_2O} + k_1\theta_{O_2^*} - k_{-1}\theta_{HOO^*} \quad \text{(S5)}$$

$$\frac{\partial \theta_{O^*}}{\partial t} = -k_3\theta_{O^*} + k_{-3}\theta_{HO^*} + k_2\theta_{HOO^*} - k_{-2}\theta_{O^*}x_{H_2O} \quad \text{(S6)}$$

$$\frac{\partial \theta_{HO^*}}{\partial t} = -k_4\theta_{HO^*} + k_{-4}\theta_* x_{H_2O} + k_3\theta_{O^*} - k_{-3}\theta_{HO^*} \quad \text{(S7)}$$

$$\frac{\partial \theta_*}{\partial t} = k_4\theta_{HO^*} - k_{-4}x_{H_2O}\theta_* - k_1\theta_* x_{O_2} + k_{-1}\theta_{HOO^*} \quad \text{(S8)}$$

Where, t, θ and x refers to the time, coverage of intermediates and mole fraction, respectively. The value of x_{H_2O} was set as 1, and x_{O_2} was set as 2.34×10^{-5}, which represents O_2(g) in equilibrium with O_2(aq) at 1 atm. The coverages of intermediates on the PM active site should satisfy the following relationship:

$$\theta_* + \theta_{O_2} + \theta_{O*} + \theta_{HO*} + \theta_{HOO*} = 1 \quad \text{(S9)}$$

The equilibrium constant (K_i) can be calculated by the following equation:

$$K_i = exp\left[-\frac{e(U - U_i)}{k_b T}\right] \quad \text{(S10)}$$

Where, k_b, T and U_i refers to the Boltzmann constant, the temperature and the reversible potential, respectively. In addition, $U_i = \Delta G_i/e$, and ΔG_i refers to the Gibbs free energy change. The rate constant (k_i) is calculated by the following equation:

$$k_i = A_i exp\left[-\frac{\Delta E_{a,i}}{k_b T}\right] exp\left[-\frac{e\beta_i(U - U_i}{k_b T}\right] \quad \text{(S11)}$$

Where, A_i refers to the pre-exponential factor set as 1.23×10^9 and β_i is the symmetry factor set as 0.5. $E_{a,i}$ is activation energy. The activation energy values of the electrochemical ORR steps are generally small, ranging from 0.10 to 0.26 eV, as reported in previous literature[5, 6]. Therefore, we used 0.26 eV value of the activation energy for all the electrochemical steps of the ORR in the work.

Moreover, the rate constant of the reverse reaction (k_{-i}) can be calculated by the following equation:

$$k_{-i} = \frac{k_i}{K_i} \quad \text{(S12)}$$

The current density (j) can be calculated by the following equation:

$$j = e\rho TOF_{e-} \quad \text{(S13)}$$

where ρ is the surface density of active sites.

4. Descriptor identification

The considered seven fundamental parameters in this work, including the Pauling electronegativity (PE) of PM atoms, the electron affinity (EA) of PM atoms, the first ionization energy (IP) of PM atoms, the p-electrons (N) of PM atoms, the atomic charge (Q_{PM}) of PM atoms before reaction, the distance between PM and N/O atoms (Dis), and the atomic radii (AR) of PM atoms.

The SISSO package[7, 8] was used to identify a simple and accurate descriptor to predict the adsorption Gibbs free energy of the key intermediates HO* (ΔG_{HO*}) according to the below

equation:

$$\Delta G_{HO*} = -686.07 \times \frac{\exp\left(\frac{EA}{AR}\right) * IP^2}{\exp(PE)} + 0.14 \times \left|\frac{\sqrt[3]{EA}\sqrt{N} * \ln M}{lnQ_{TM}} - lnAR * \sqrt[3]{IP}\right| - 0.06 \times \left|\frac{ex}{ln} \right.$$
$$lnN + 3.33$$

5. Computational methods

All the spin-polarized density functional theory calculations were carried out by using the Vienna ab initio Simulation Package (VASP).[9-10] The interactions between ion cores and valence electrons were described by using the projector augmented wave (PAW) method.[11] The electronic exchange-correlation interactions were calculated by using the Perdew-Burke-Ernzerhof (PBE)[12] functional of the generalized gradient approximation (GGA).[13] The Van der Waals (vdW) interactions were described by using the dispersion-corrected DFT-D3 method.[14] The plane-wave cutoff energy was set to 500 eV, and the convergence criterion for energy and force during geometrical optimization was set to 10^{-5} eV and 10^{-2} eV/Å, respectively. The Brillouin zone was sampled using a 3 x 3 x 1 k-point[15] during geometry optimization. The vacuum space of 20 Å was adopted to avoid the interaction between the periodic images. The solvent effect was implicitly considered by using the VASPsol code to simulate the water solvent environment.[16] Ab initio molecular dynamics (AIMD) simulations were performed to demonstrate the thermodynamic stability of catalyst, and the algorithm of the Nose thermostat was carried out to simulate a canonical ensemble[17] for 10 ps with a time step of 1 fs. Bader charge analysis was performed to investigate the charge transfer process.[18] The calculation details for the ORR is listed in the Supporting Information as in our previous study.[19] The adsorption Gibbs free energy is defined as $G_{ads} = G_{adsorbent+catalyst} - G_{catalyst} - G_{adsorbent}$, here $G_{adsorbent+catalyst}$, $G_{catalyst}$, and $G_{adsorbent}$ is the Gibbs free energy of the adsorbent on the catalyst, the isolated catalyst, and the isolated adsorbent, respectively.

The E_f and U_{diss} defined as $E_f = (E_{PMNxO4-x} - E_{NxO4-x} - 3E_{PM})/3$ and $U_{diss} = U_{diss}^{\circ}$ (bulk) - E_f/ne, respectively. Where $E_{PMNxO4-x}$ and E_{NxO4-x} denote the total energies of PMN_xO_{4-x} system and N_xO_{4-x} substrate, respectively. E_{PM} denote the total energy of a metal atom in its most stable bulk structure. U_{diss}° (bulk) represents the standard dissolution potential of bulk metal, n refers to the number of electrons involved during the dissolution process. Since E_{PM} is referenced with respect to its corresponding bulk metal, the designed catalysts with negative values of E_f

($E_f < 0$) are evaluated to be thermodynamically stable against the clustering of PM atoms. The designed catalysts with positive values of U_{diss} ($U_{diss} < 0$) vs standard hydrogen electrode (SHE) are regarded as electrochemically stable.

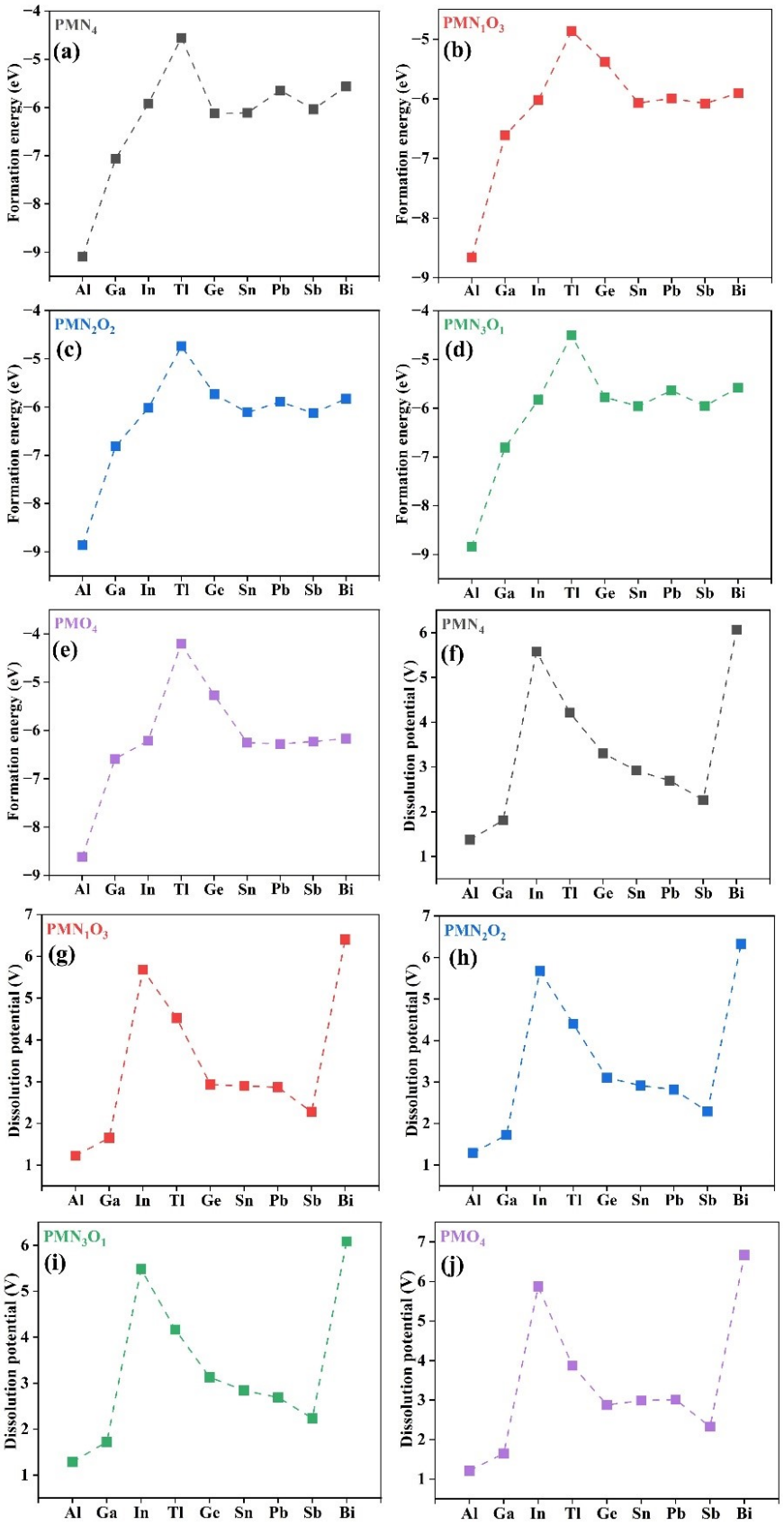

Fig. S1 Calculated formation energy (a-e) and dissolution potential of metal atoms (f-j) for the designed PMN_xO_{4-x}-HADQ catalysts.

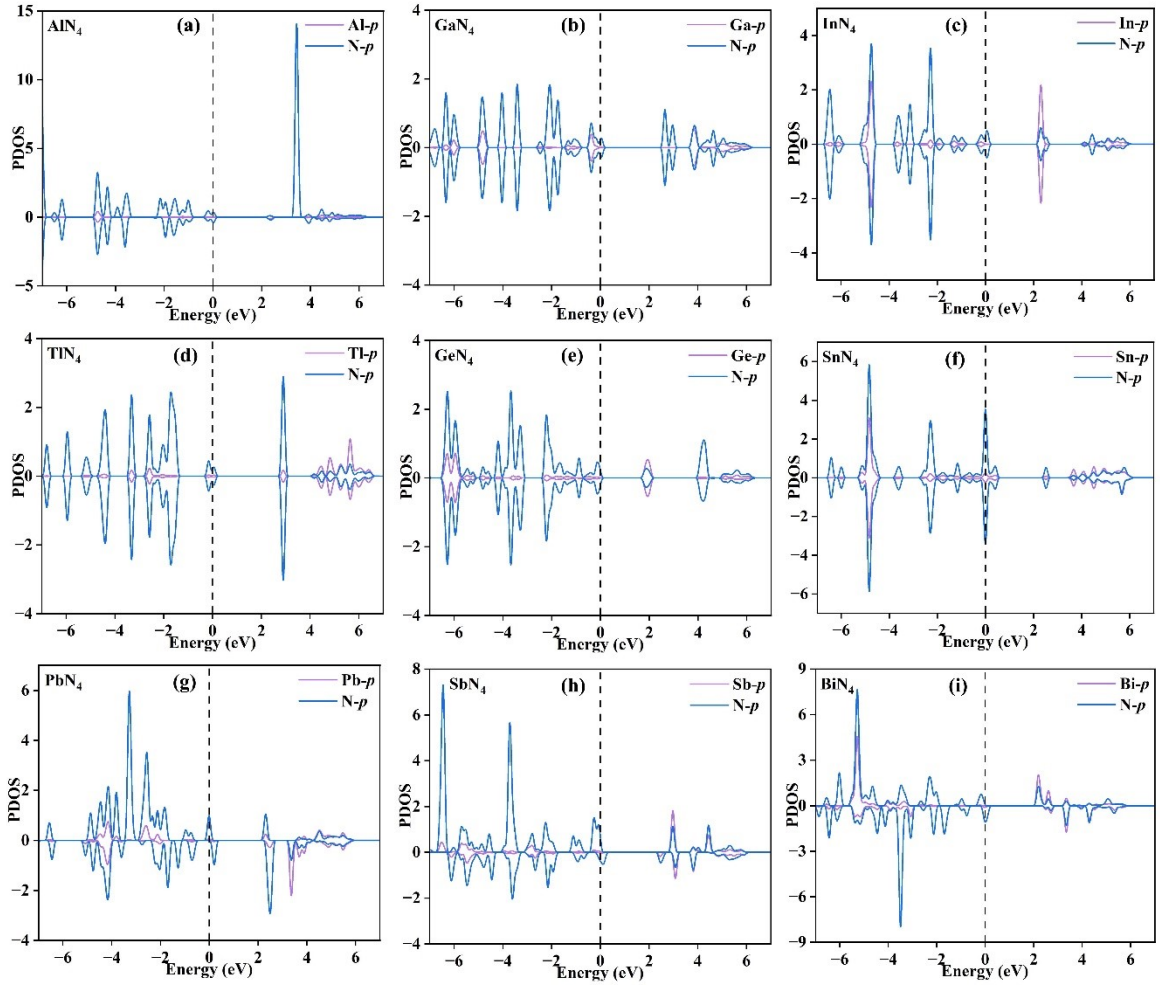

Fig. S2 Calculated partial density of states (PDOS) for the *p* orbitals of N atoms and PM atoms for the designed PMN_4-HADQ catalysts. The Fermi level is set at the zero of energy (dashed line in figures).

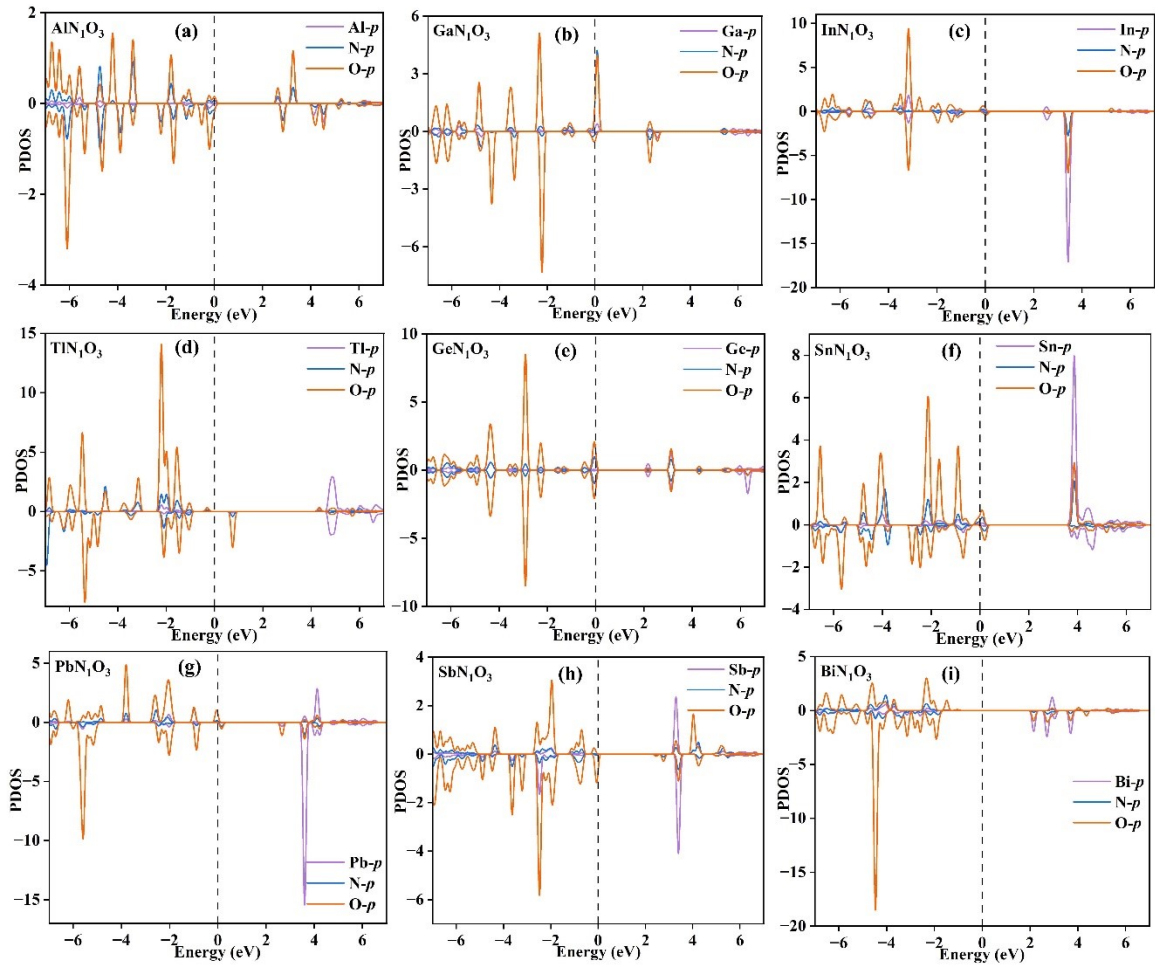

Fig. S3 Calculated partial density of states (PDOS) for the *p* orbitals of N/O atoms and PM atoms for the designed PMN_1O_3-HADQ catalysts. The Fermi level is set at the zero of energy (dashed line in figures).

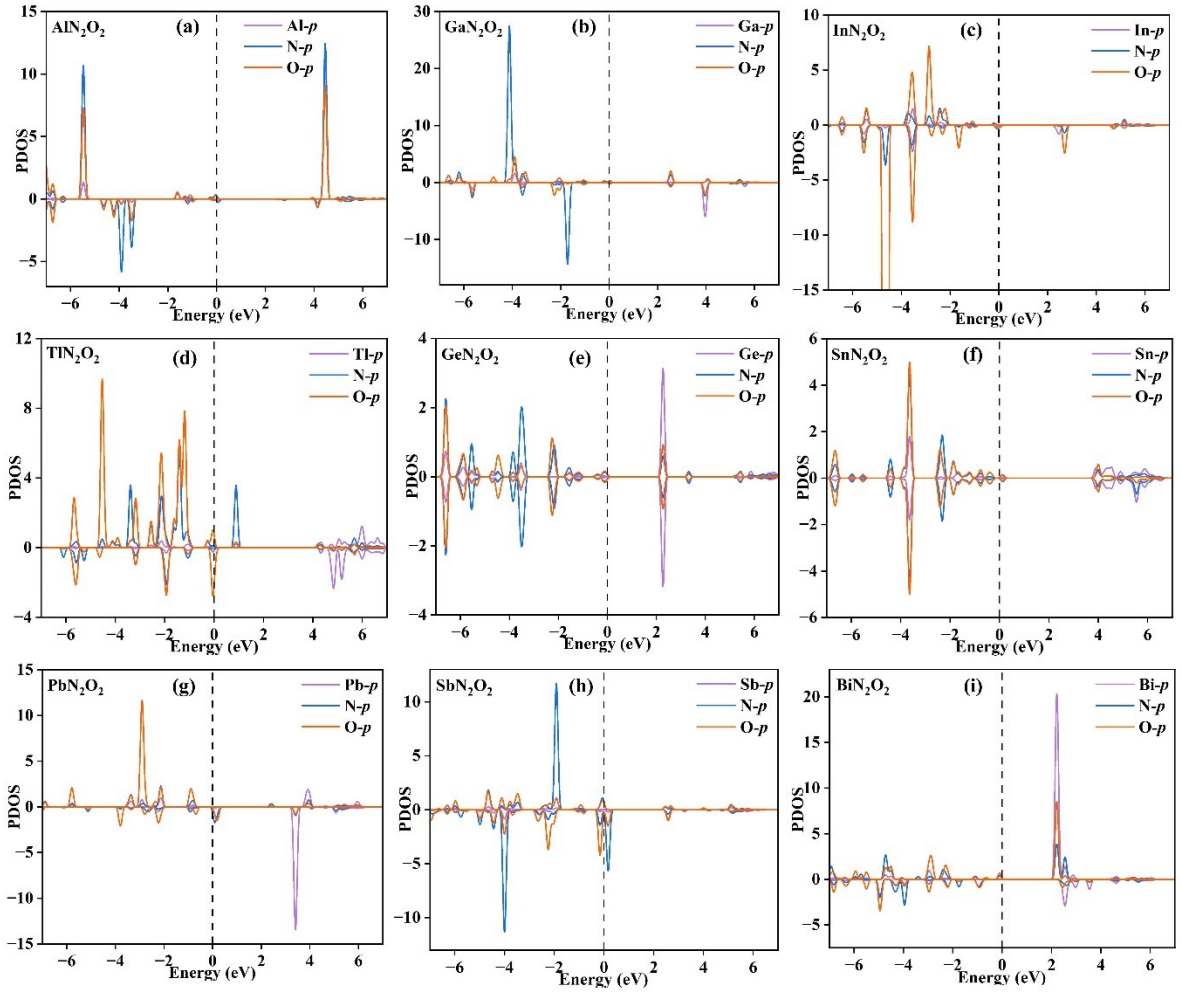

Fig. S4 Calculated partial density of states (PDOS) for the *p* orbitals of N/O atoms and PM atoms for the designed PMN_2O_2-HADQ catalysts. The Fermi level is set at the zero of energy (dashed line in figures).

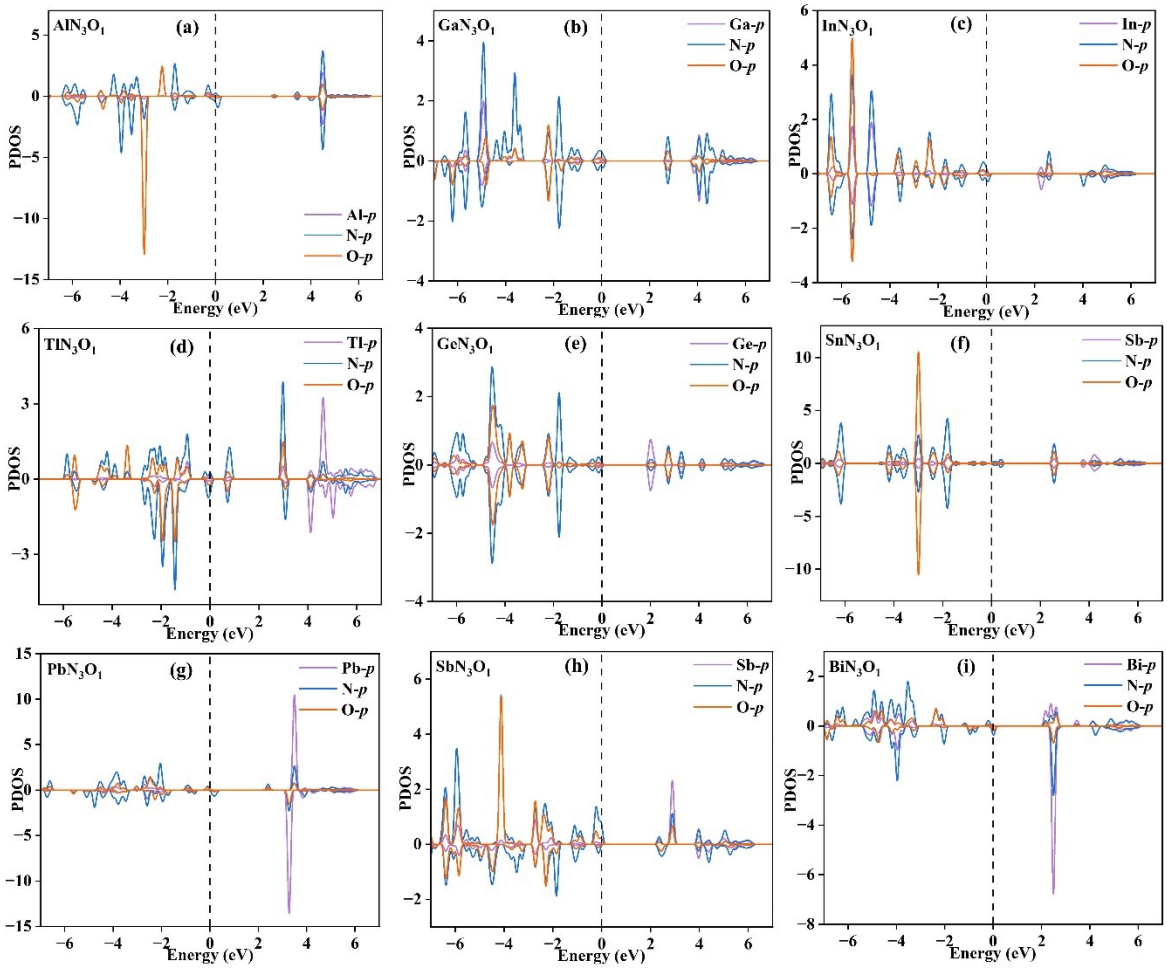

Fig. S5 Calculated partial density of states (PDOS) for the *p* orbitals of N/O atoms and PM atoms for the designed PMN_3O_1-HADQ catalysts. The Fermi level is set at the zero of energy (dashed line in figures).

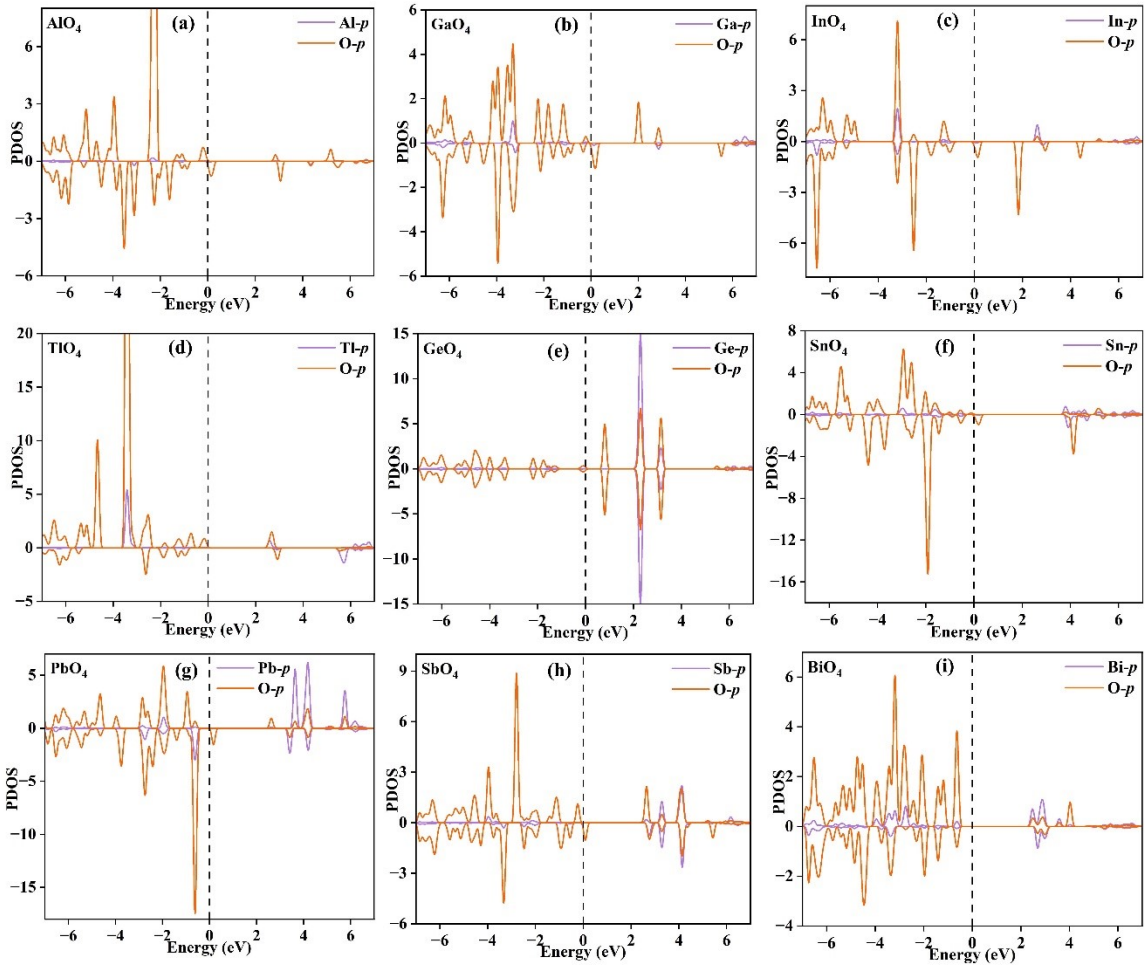

Fig. S6 Calculated partial density of states (PDOS) for the *p* orbitals of O atoms and PM atoms for the designed PMO_4-HADQ catalysts. The Fermi level is set at the zero of energy (dashed line in figures).

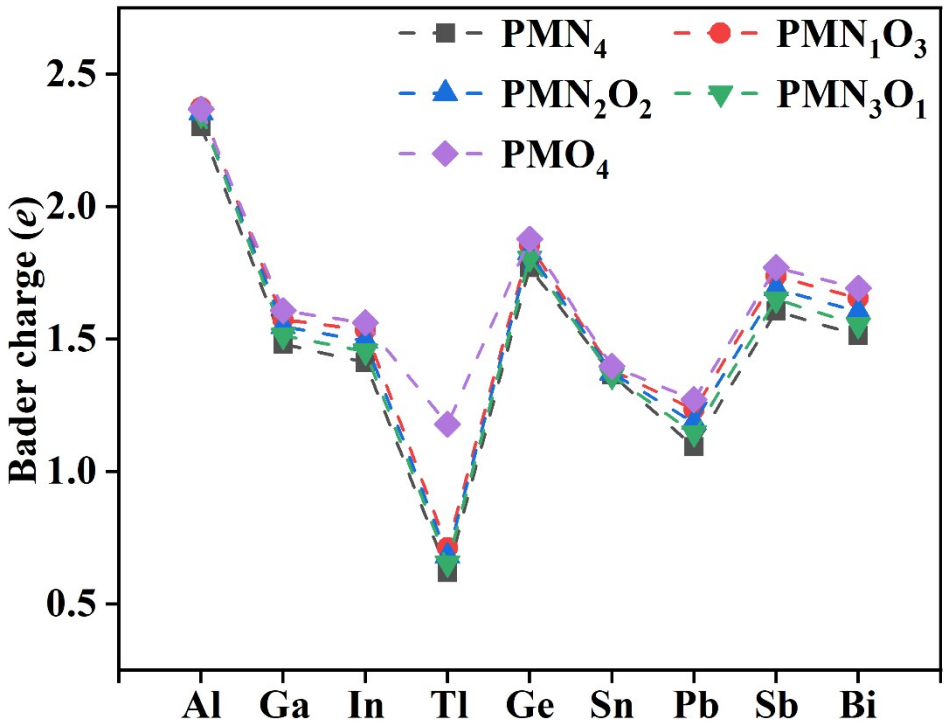

Fig. S7 Calculated charge transfer from metal atoms to substrates of all the designed PMN_xO_{4-x}-HADQ catalysts based on Bader charge analysis. The positive value of Bader charge suggests that the charge is transferred from metal atoms to the substrates.

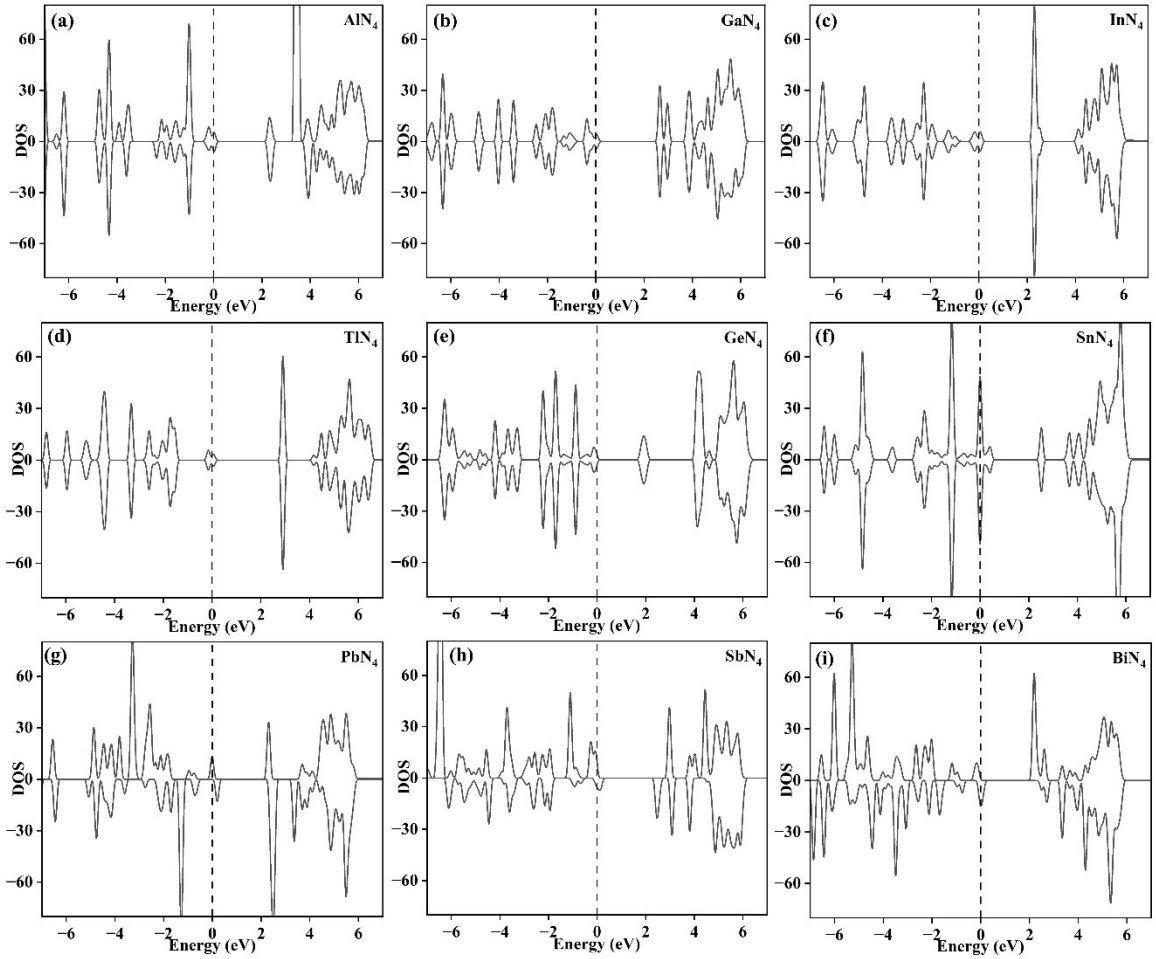

Fig. S8 Calculated density of states (DOS) for the designed PMN_4-HADQ catalysts. The Fermi level is set at the zero of energy (dashed line in figures).

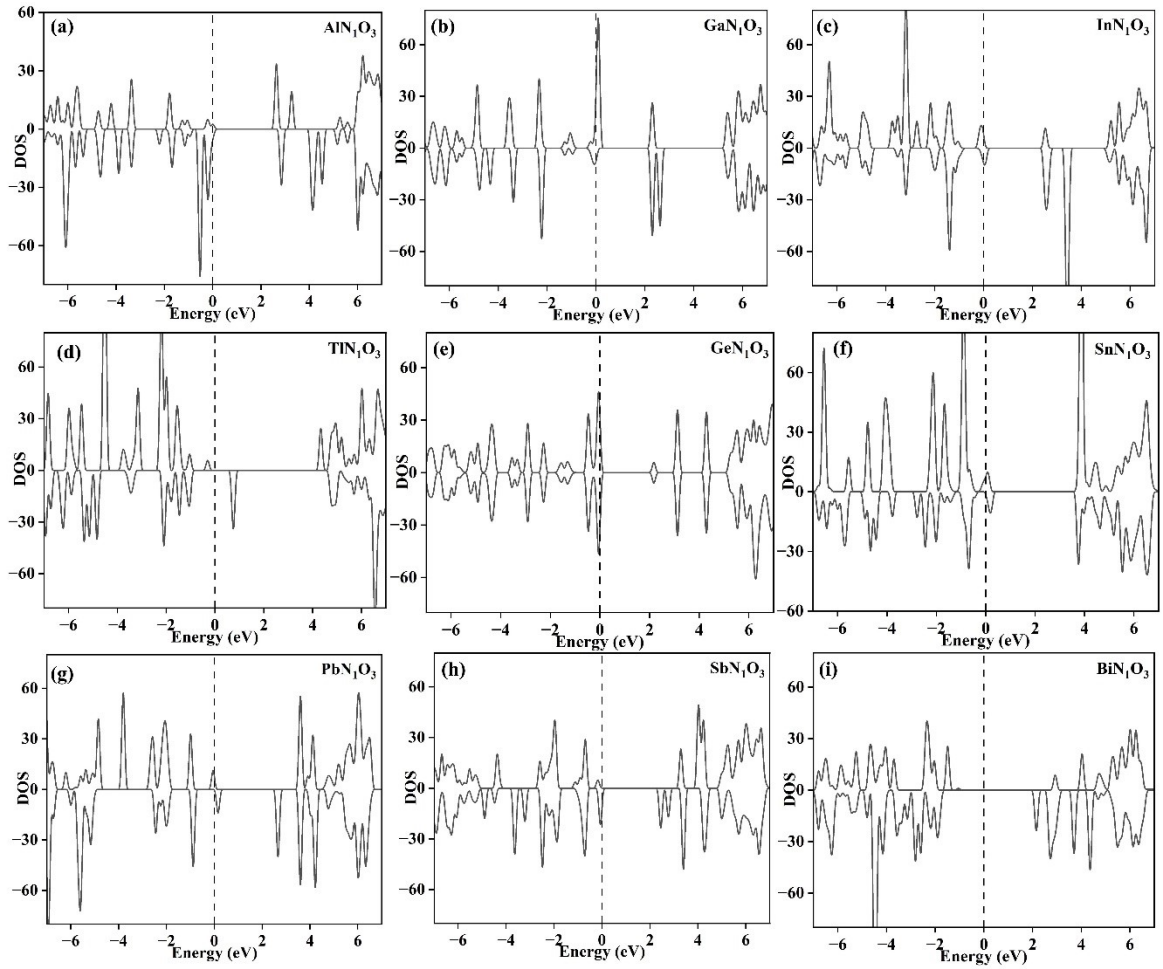

Fig. S9 Calculated density of states (DOS) for the designed PMN_1O_3-HADQ catalysts. The Fermi level is set at the zero of energy (dashed line in figures).

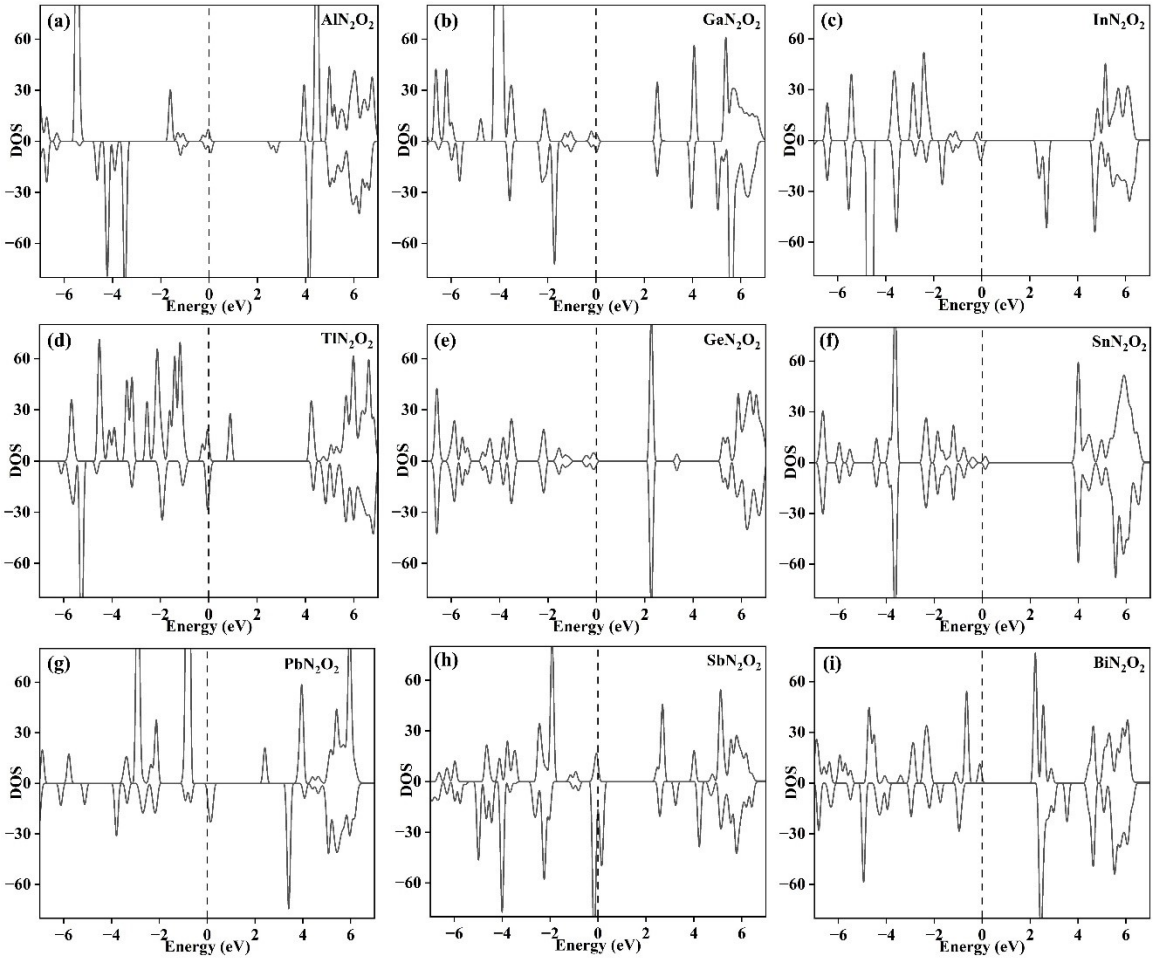

Fig. S10 Calculated density of states (DOS) for the designed PMN_2O_2-HADQ catalysts. The Fermi level is set at the zero of energy (dashed line in figures).

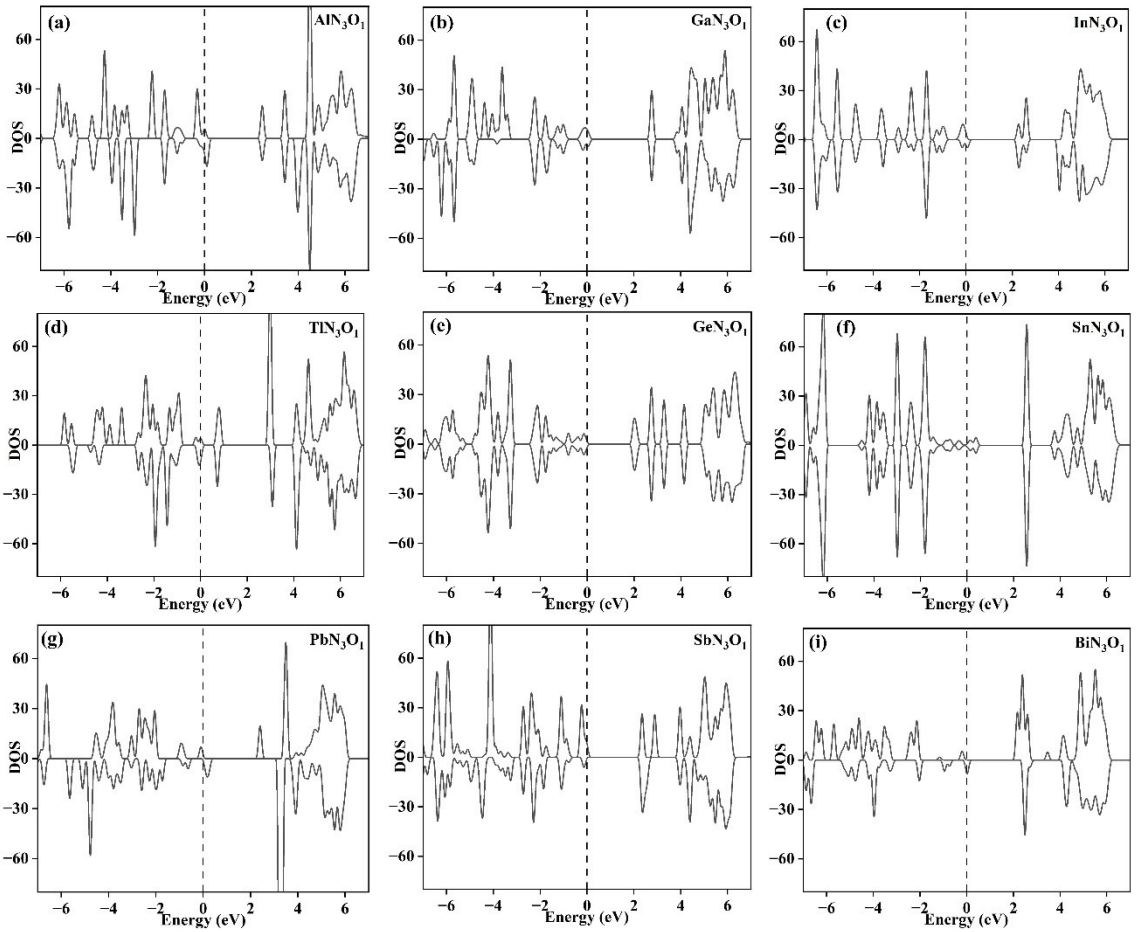

Fig. S11 Calculated density of states (DOS) for the designed PMN_3O_1-HADQ catalysts. The Fermi level is set at the zero of energy (dashed line in figures).

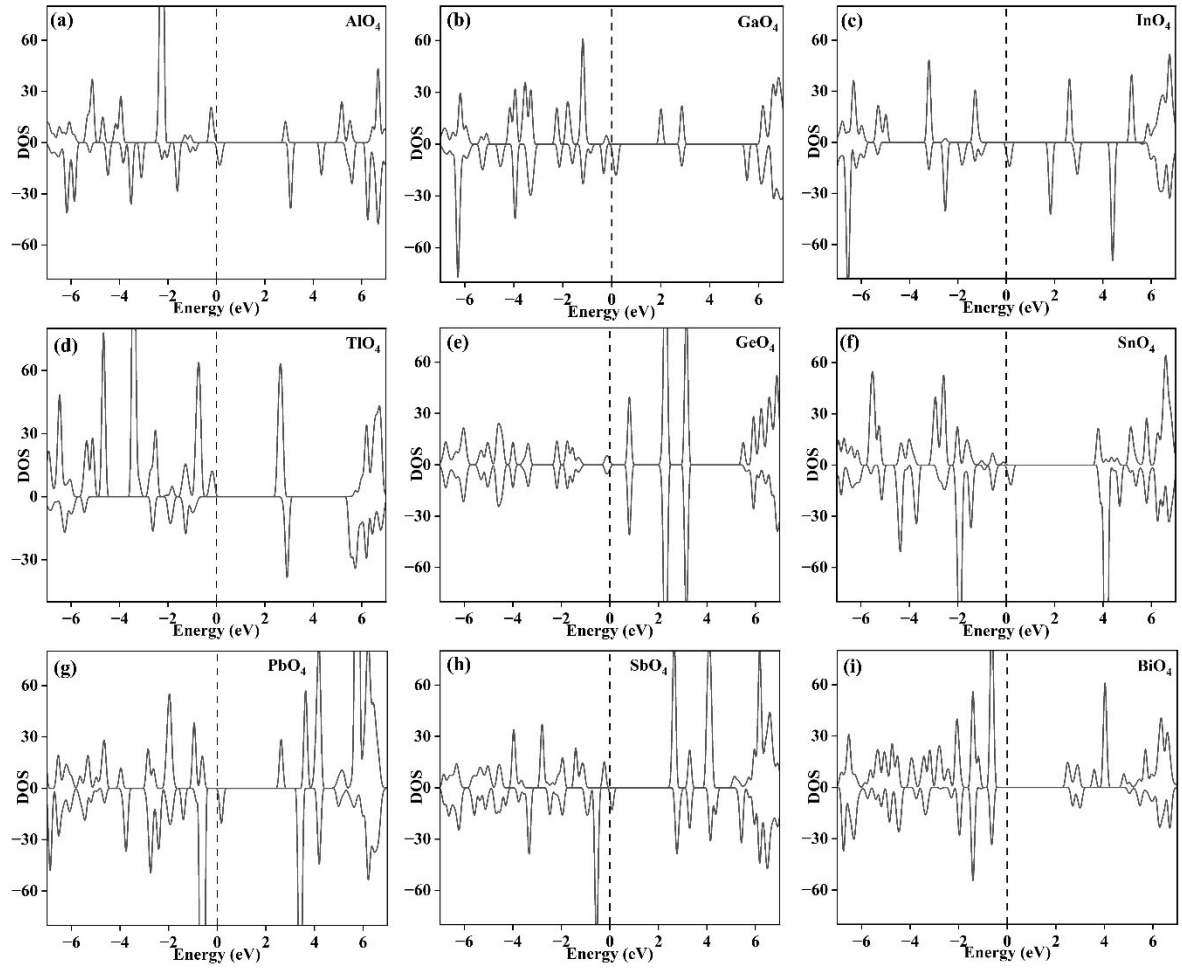

Fig. S12 Calculated density of states (DOS) for the designed PMO_4-HADQ catalysts. The Fermi level is set at the zero of energy (dashed line in figures).

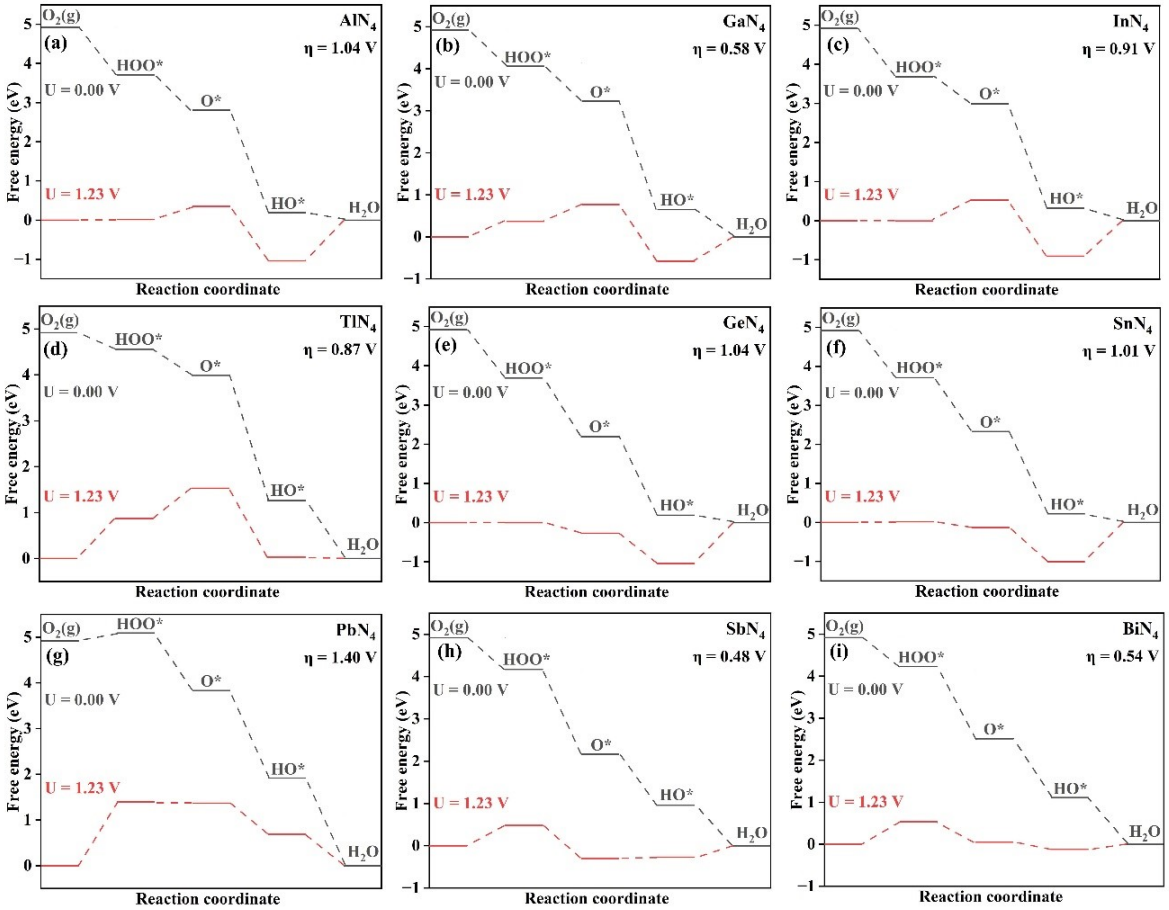

Fig. S13 Calculated free energy diagrams of ORR on the designed PMN_4-HADQ catalysts at U = 0 V (grey) and U = 1.23 V (red) under acid conditions.

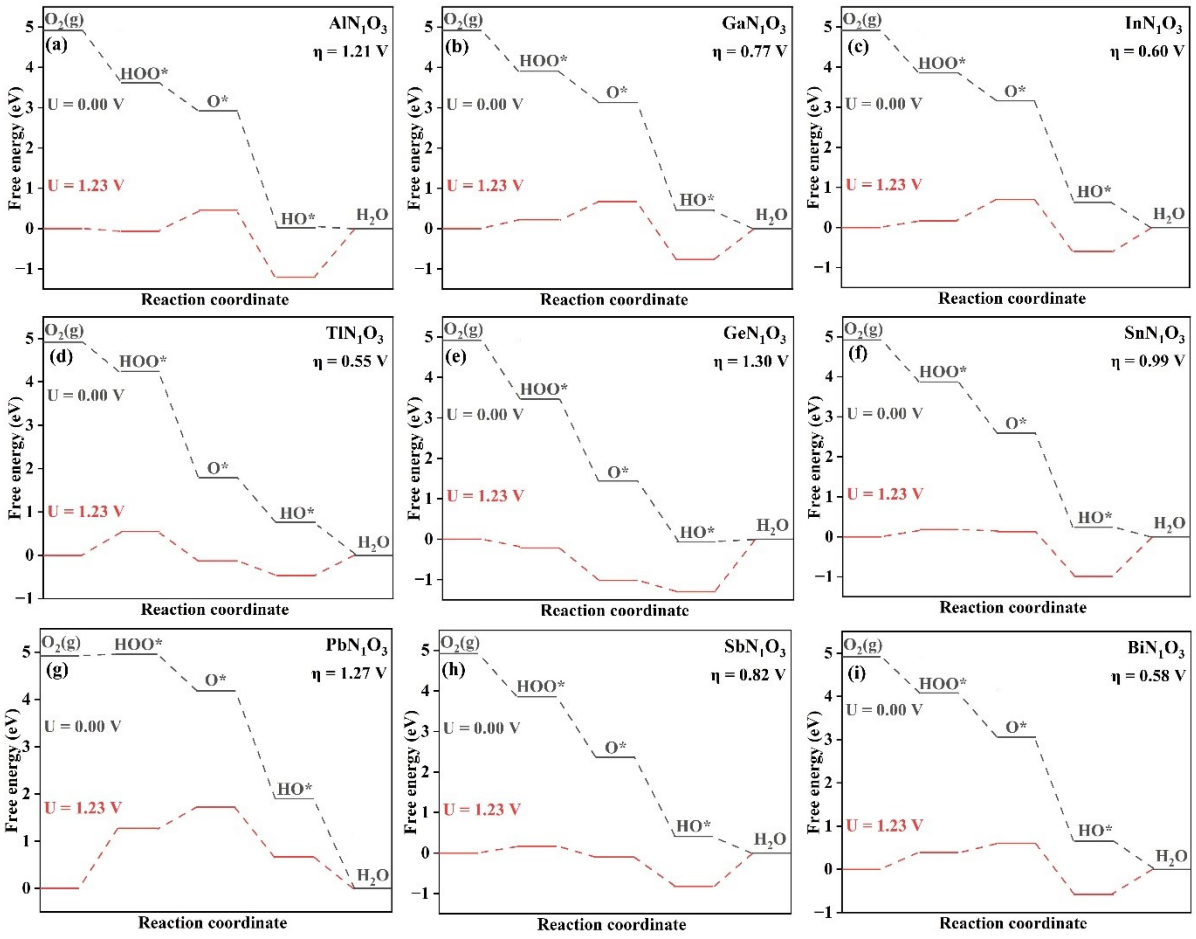

Fig. S14 Calculated free energy diagrams of ORR on the designed PMN_1O_3-HADQ catalysts at U = 0 V (grey) and U = 1.23 V (red) under acid conditions.

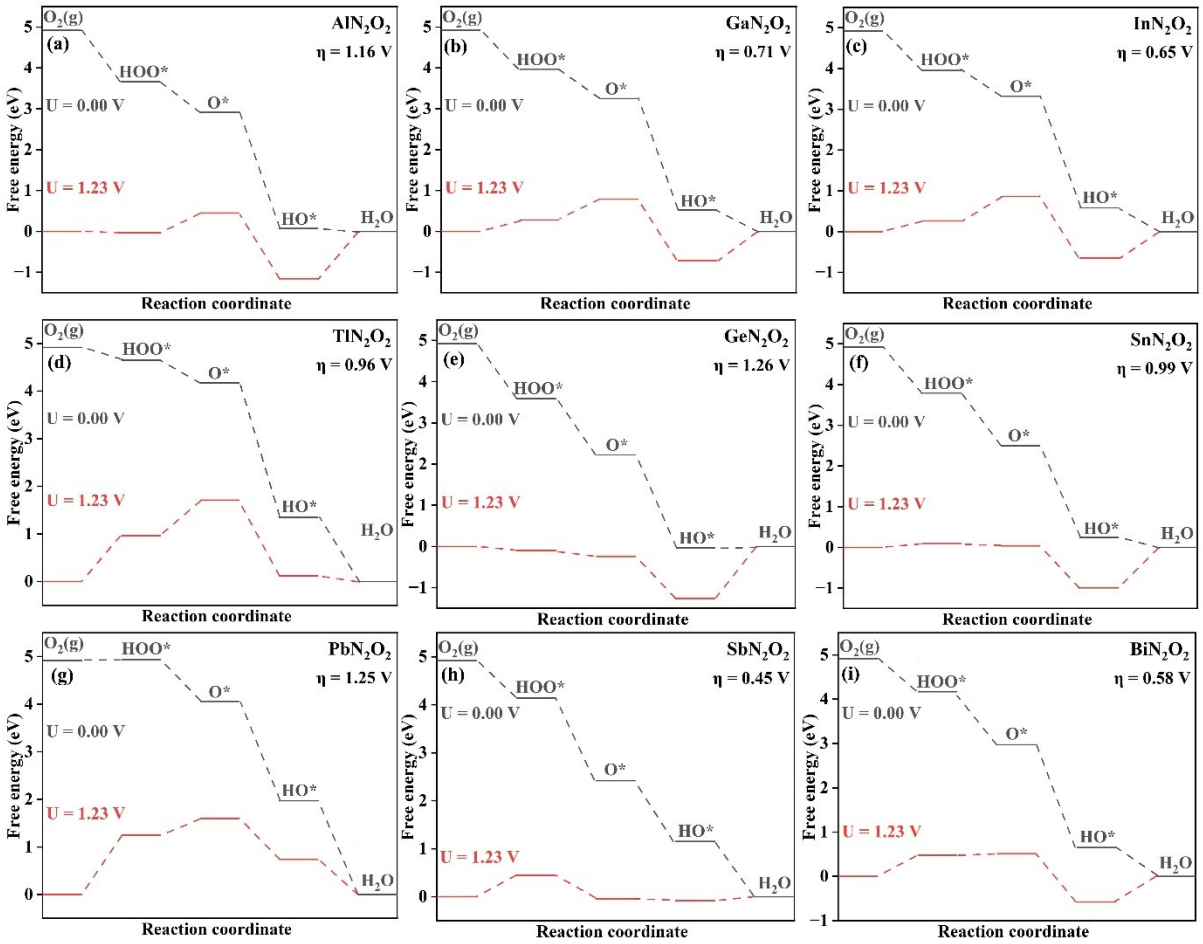

Fig. S15 Calculated free energy diagrams of ORR on the designed PMN_2O_2-HADQ catalysts at U = 0 V (grey) and U = 1.23 V (red) under acid conditions.

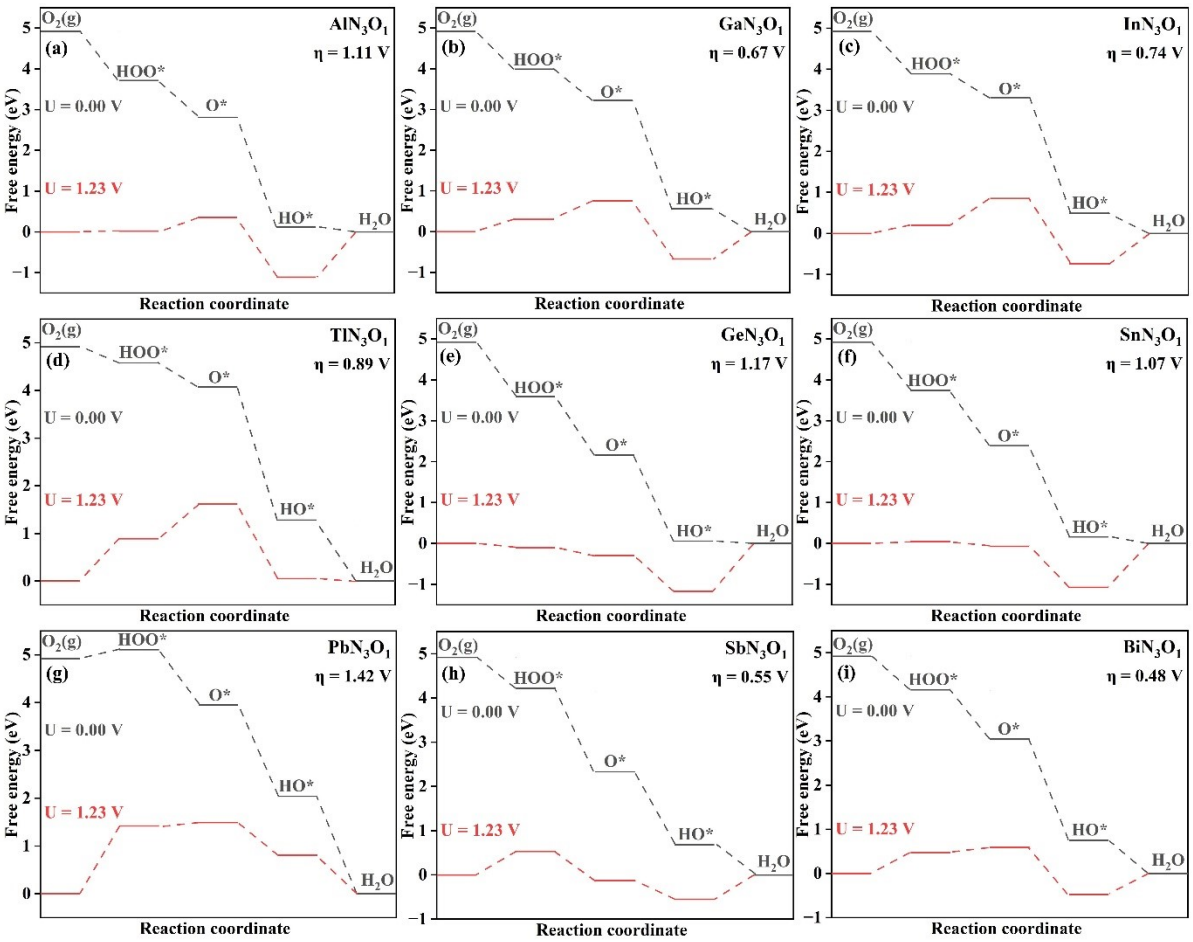

Fig. S16 Calculated free energy diagrams of ORR on the designed PMN_3O_1-HADQ catalysts at U = 0 V (grey) and U = 1.23 V (red) under acid conditions.

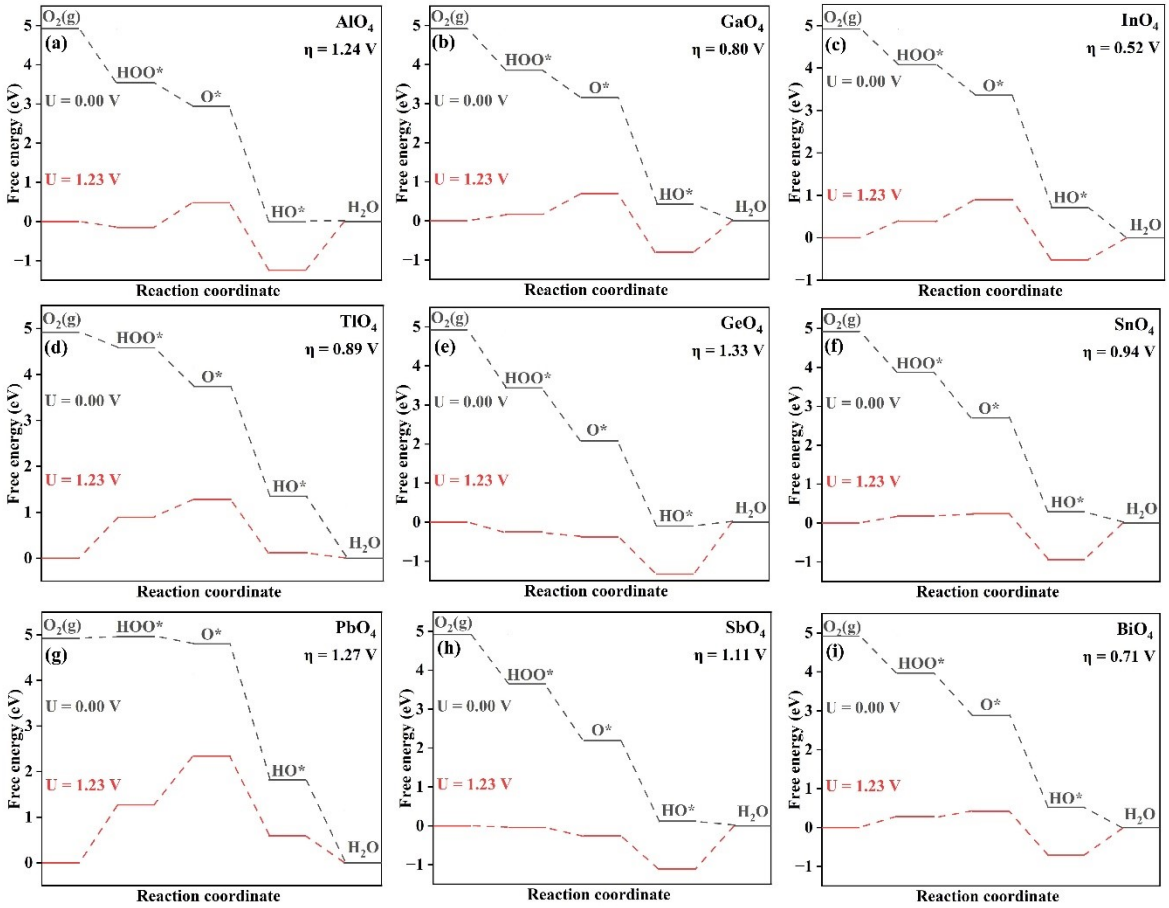

Fig. S17 Calculated free energy diagrams of ORR on the designed PMO_4-HADQ catalysts at U = 0 V (grey) and U = 1.23 V (red) under acid conditions.

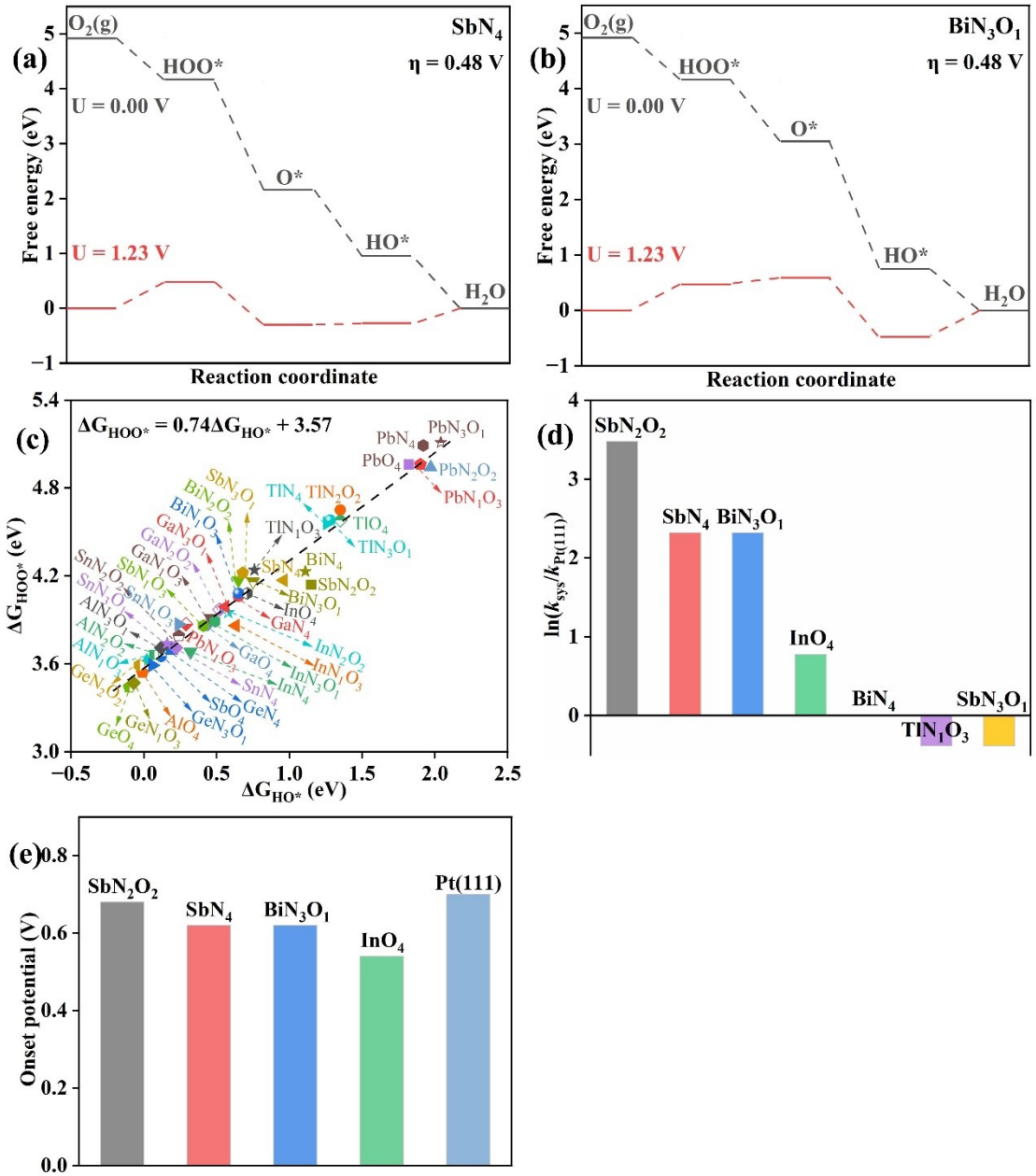

Fig. S18 Calculated free energy diagrams of promising catalysts for the ORR (a) SbN_4-HADQ, and (b) BiN_3O_1-HADQ, respectively. (c) Scaling relationship between ΔG_{HO*} and ΔG_{HOO*} on all the designed PMN_xO_{4-x}-HADQ catalysts. (d) Variation activity of the potential ORR electrocatalysts. (e) The corresponding half-wave potential of SbN_2O_2-HADQ, SbN_4-HADQ, BiN_3O_1-HADQ, InO_4-HADQ and Pt (111).

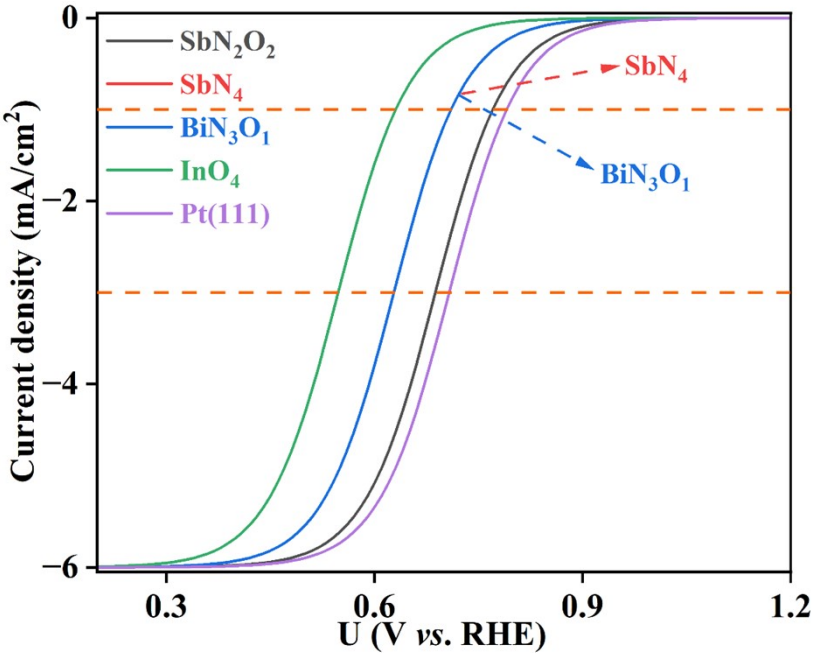

Fig. S19 Theoretical polarization curves of SbN_2O_2-HADQ, SbN_4-HADQ, BiN_3O_1-HADQ, InO_4-HADQ and Pt (111).

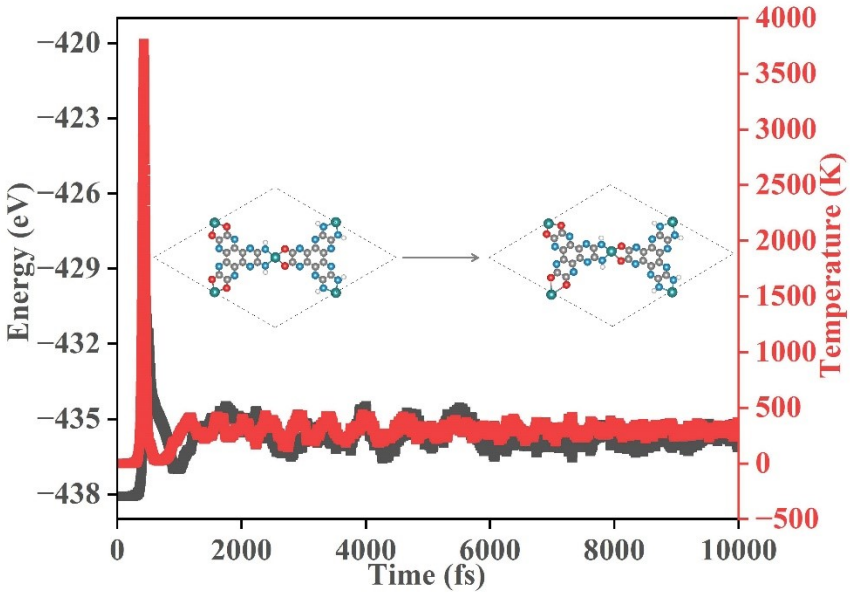

Fig. S20 Evolution of the total energy and temperature for the SbN_2O_2-HADQ, the time lasts for 10 ps at 300 K. The initial and final atomic configurations during the AIMD simulation are inserted.

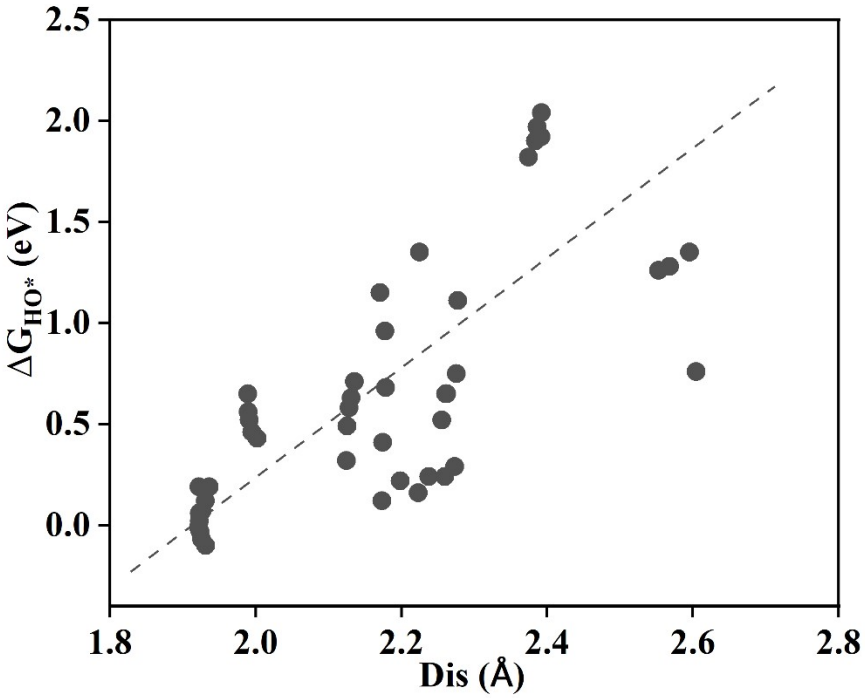

Fig. S21 Relationship between the adsorption Gibbs free energies of the key intermediate HO* and the distance between PM and N/O atoms.

Table S1 The feature values for descriptor identification study.

System	AR	PE	Q_{PM}	EA	IP	N	Dis
Al-N_4	3.42	13.77	2.3031	0.441	64.104	13	1.936
Ga-N_4	3.6	13.97	1.4805	0.43	64.12	13	1.989
Ge-N_4	3.49	14.17	1.7704	1.23	66	14	1.922
In-N_4	3.8	13.94	1.4125	0.3	64.905	13	2.124
Sn-N_4	3.69	14.12	1.3646	1.11	65.462	14	2.198
Sb-N_4	3.57	14.21	1.6052	1.07	66.759	15	2.177
Tl-N_4	3.8	13.78	0.6186	0.2	64.226	13	2.553
Pb-N_4	3.78	14.49	1.0929	0.36	65.535	14	2.392
Bi-N_4	3.67	14.18	1.5131	0.946	65.407	15	2.277
Al-O_4	3.1	15.37	2.3677	6.285	60.44	17	1.922
Ga-O_4	3.28	15.57	1.6065	6.274	60.456	17	2.002
Ge-O_4	3.17	15.77	1.8773	7.074	62.336	18	1.931
In-O_4	3.48	15.54	1.5608	6.144	61.241	17	2.136
Sn-O_4	3.37	15.72	1.3969	6.954	61.798	18	2.273
Sb-O_4	3.25	15.81	1.7693	6.914	63.095	19	2.173
Tl-O_4	3.48	15.38	1.1773	6.044	60.562	17	2.225
Pb-O_4	3.46	16.09	1.2712	6.204	61.871	18	2.375
Bi-O_4	3.35	15.78	1.692	6.79	61.743	19	2.255
Al-N_1O_3	3.18	14.97	2.3739	4.824	61.356	16	1.923
Ga-N_1O_3	3.36	15.17	1.5736	4.813	61.372	16	1.995
Ge-N_1O_3	3.25	15.37	1.855	5.613	63.252	17	1.926
In-N_1O_3	3.56	15.14	1.5338	4.683	62.157	16	2.131
Sn-N_1O_3	3.45	15.32	1.3817	5.493	62.714	17	2.259
Sb-N_1O_3	3.33	15.41	1.7376	5.453	64.011	18	2.174
Tl-N_1O_3	3.56	14.98	0.7116	4.583	61.478	16	2.604
Pb-N_1O_3	3.54	15.69	1.2331	4.743	62.787	17	2.384
Bi-N_1O_3	3.43	15.38	1.654	5.329	62.659	18	2.261

Al-N_2O_2	3.26	14.57	2.3533	3.363	62.272	15	1.926
Ga-N_2O_2	3.44	14.77	1.5477	3.352	62.288	15	1.991
Ge-N_2O_2	3.33	14.97	1.8262	4.152	64.168	16	1.924
In-N_2O_2	3.64	14.74	1.4918	3.222	63.073	15	2.128
Sn-N_2O_2	3.53	14.92	1.3723	4.032	63.63	16	2.238
Sb-N_2O_2	3.41	15.01	1.6902	3.992	64.927	17	2.171
Tl-N_2O_2	3.64	14.58	0.6794	3.122	62.394	15	2.595
Pb-N_2O_2	3.62	15.29	1.1846	3.282	63.703	16	2.386
Bi-N_2O_2	3.51	14.98	1.6029	3.868	63.575	17	2.262
Al-N_3O_1	3.34	14.17	2.3492	1.902	63.188	14	1.931
Ga-N_3O_1	3.52	14.37	1.5129	1.891	63.204	14	1.989
Ge-N_3O_1	3.41	14.57	1.8047	2.691	65.084	15	1.922
In-N_3O_1	3.72	14.34	1.4533	1.761	63.989	14	2.126
Sn-N_3O_1	3.61	14.52	1.3613	2.571	64.546	15	2.223
Sb-N_3O_1	3.49	14.61	1.65	2.531	65.843	16	2.178
Tl-N_3O_1	3.72	14.18	0.6528	1.661	63.31	14	2.568
Pb-N_3O_1	3.70	14.89	1.1447	1.821	64.619	15	2.392
Bi-N_3O_1	3.59	14.58	1.5529	2.407	64.491	16	2.275

The coordination of the designed promising PMN_xO_{4-x}-HADQ ORR catalysts

```
#======================================================================
# CRYSTAL DATA
#----------------------------------------------------------------------
data_VESTA_phase_1
_pd_phase_name                         'SbN2O2                        '
_cell_length_a                         21.89000
_cell_length_b                         21.89000
_cell_length_c                         20.00000
_cell_angle_alpha                      90
_cell_angle_beta                       90
_cell_angle_gamma                      120
_symmetry_space_group_name_H-M         'P 1'
_symmetry_Int_Tables_number            1
```

```
loop_
_symmetry_equiv_pos_as_xyz
   'x, y, z'

loop_
   _atom_site_label
   _atom_site_occupancy
   _atom_site_fract_x
   _atom_site_fract_y
   _atom_site_fract_z
   _atom_site_adp_type
   _atom_site_B_iso_or_equiv
   _atom_site_type_symbol
   H1    1.0   0.566107   0.645554   0.202764   Biso   1.000000 H
   H2    1.0   0.643847   0.077382   0.202014   Biso   1.000000 H
   H3    1.0   0.918924   0.565748   0.203157   Biso   1.000000 H
   H4    1.0   0.354556   0.433911   0.202438   Biso   1.000000 H
   H5    1.0   0.922591   0.356088   0.201991   Biso   1.000000 H
   H6    1.0   0.434232   0.081087   0.203244   Biso   1.000000 H
   N1    1.0   0.480950   0.081188   0.200992   Biso   1.000000 N
   N2    1.0   0.920780   0.401788   0.200398   Biso   1.000000 N
   N3    1.0   0.400782   0.480986   0.200340   Biso   1.000000 N
   N4    1.0   0.918776   0.519000   0.200946   Biso   1.000000 N
   N5    1.0   0.598132   0.079171   0.200386   Biso   1.000000 N
   N6    1.0   0.519065   0.599302   0.200524   Biso   1.000000 N
   N7    1.0   0.667492   0.204602   0.195263   Biso   1.000000 N
   N8    1.0   0.333138   0.794775   0.195247   Biso   1.000000 N
   N9    1.0   0.793777   0.461725   0.195647   Biso   1.000000 N
   N10   1.0   0.204224   0.537194   0.196623   Biso   1.000000 N
   N11   1.0   0.537511   0.333169   0.196265   Biso   1.000000 N
   N12   1.0   0.462440   0.667804   0.195802   Biso   1.000000 N
   N13   1.0   0.205391   0.667038   0.195413   Biso   1.000000 N
   N14   1.0   0.795354   0.332454   0.195251   Biso   1.000000 N
   N15   1.0   0.462913   0.795807   0.196865   Biso   1.000000 N
   N16   1.0   0.538213   0.206190   0.195675   Biso   1.000000 N
   N17   1.0   0.332231   0.537600   0.195635   Biso   1.000000 N
   N18   1.0   0.666622   0.462328   0.196045   Biso   1.000000 N
   O1    1.0   0.520092   0.918537   0.201977   Biso   1.000000 O
   O2    1.0   0.082987   0.602589   0.200839   Biso   1.000000 O
   O3    1.0   0.601496   0.519863   0.201379   Biso   1.000000 O
   O4    1.0   0.081484   0.480132   0.201593   Biso   1.000000 O
   O5    1.0   0.397677   0.917182   0.200489   Biso   1.000000 O
   O6    1.0   0.479938   0.398224   0.201625   Biso   1.000000 O
   C1    1.0   0.539140   0.145207   0.197277   Biso   1.000000 C
```

C2	1.0	0.461126	0.855094	0.198129	Biso	1.000000 C
C3	1.0	0.855245	0.394007	0.197031	Biso	1.000000 C
C4	1.0	0.145248	0.605741	0.197309	Biso	1.000000 C
C5	1.0	0.605371	0.460823	0.197648	Biso	1.000000 C
C6	1.0	0.393978	0.538944	0.197114	Biso	1.000000 C
C7	1.0	0.144959	0.539037	0.197921	Biso	1.000000 C
C8	1.0	0.854753	0.460787	0.197264	Biso	1.000000 C
C9	1.0	0.394458	0.854867	0.197187	Biso	1.000000 C
C10	1.0	0.605924	0.144708	0.197033	Biso	1.000000 C
C11	1.0	0.461080	0.606041	0.197197	Biso	1.000000 C
C12	1.0	0.538986	0.394409	0.197760	Biso	1.000000 C
C13	1.0	0.600424	0.266887	0.194251	Biso	1.000000 C
C14	1.0	0.400089	0.733712	0.194720	Biso	1.000000 C
C15	1.0	0.733366	0.332965	0.193965	Biso	1.000000 C
C16	1.0	0.266604	0.665623	0.194228	Biso	1.000000 C
C17	1.0	0.665416	0.399552	0.194518	Biso	1.000000 C
C18	1.0	0.333108	0.599829	0.194381	Biso	1.000000 C
C19	1.0	0.266363	0.600006	0.194646	Biso	1.000000 C
C20	1.0	0.733069	0.399517	0.194221	Biso	1.000000 C
C21	1.0	0.334506	0.733532	0.194177	Biso	1.000000 C
C22	1.0	0.667001	0.266602	0.193976	Biso	1.000000 C
C23	1.0	0.400221	0.666943	0.194445	Biso	1.000000 C
C24	1.0	0.600323	0.334467	0.194587	Biso	1.000000 C
Sb1	1.0	0.498574	0.996819	0.240703	Biso	1.000000 Sb
Sb2	1.0	0.003126	0.501377	0.240626	Biso	1.000000 Sb
Sb3	1.0	0.501451	0.498525	0.240719	Biso	1.000000 Sb

```
#======================================================================
# CRYSTAL DATA
#----------------------------------------------------------------------
data_VESTA_phase_1
_pd_phase_name                         'SbN4                                '
_cell_length_a                         21.89000
_cell_length_b                         21.89000
_cell_length_c                         20.00000
_cell_angle_alpha                      90
_cell_angle_beta                       90
_cell_angle_gamma                        120
_symmetry_space_group_name_H-M           'P 1'
_symmetry_Int_Tables_number              1

loop_
_symmetry_equiv_pos_as_xyz
   'x, y, z'
```

```
loop_
    _atom_site_label
    _atom_site_occupancy
    _atom_site_fract_x
    _atom_site_fract_y
    _atom_site_fract_z
    _atom_site_adp_type
    _atom_site_B_iso_or_equiv
    _atom_site_type_symbol
    H1      1.0     0.565046    0.645948    0.195504    Biso    1.000000 H
    H2      1.0     0.434946    0.354041    0.195518    Biso    1.000000 H
    H3      1.0     0.354004    0.919065    0.195776    Biso    1.000000 H
    H4      1.0     0.646015    0.080943    0.195783    Biso    1.000000 H
    H5      1.0     0.081057    0.434963    0.195057    Biso    1.000000 H
    H6      1.0     0.918977    0.565038    0.195025    Biso    1.000000 H
    H7      1.0     0.646056    0.565045    0.195131    Biso    1.000000 H
    H8      1.0     0.353913    0.434968    0.195167    Biso    1.000000 H
    H9      1.0     0.919109    0.354043    0.195511    Biso    1.000000 H
    H10     1.0     0.080865    0.645928    0.195473    Biso    1.000000 H
    H11     1.0     0.434955    0.080935    0.195785    Biso    1.000000 H
    H12     1.0     0.565061    0.919071    0.195793    Biso    1.000000 H
    N1      1.0     0.481294    0.080620    0.200164    Biso    1.000000 N
    N2      1.0     0.518716    0.919376    0.200169    Biso    1.000000 N
    N3      1.0     0.919404    0.400718    0.199471    Biso    1.000000 N
    N4      1.0     0.080591    0.599265    0.199426    Biso    1.000000 N
    N5      1.0     0.599368    0.518709    0.199279    Biso    1.000000 N
    N6      1.0     0.400611    0.481294    0.199317    Biso    1.000000 N
    N7      1.0     0.080675    0.481284    0.199245    Biso    1.000000 N
    N8      1.0     0.919336    0.518706    0.199233    Biso    1.000000 N
    N9      1.0     0.400656    0.919380    0.200164    Biso    1.000000 N
    N10     1.0     0.599361    0.080626    0.200141    Biso    1.000000 N
    N11     1.0     0.518669    0.599275    0.199477    Biso    1.000000 N
    N12     1.0     0.481320    0.400721    0.199487    Biso    1.000000 N
    N13     1.0     0.667789    0.205605    0.205294    Biso    1.000000 N
    N14     1.0     0.332219    0.794396    0.205297    Biso    1.000000 N
    N15     1.0     0.794378    0.462155    0.204924    Biso    1.000000 N
    N16     1.0     0.205636    0.537855    0.204928    Biso    1.000000 N
    N17     1.0     0.537810    0.332236    0.205051    Biso    1.000000 N
    N18     1.0     0.462186    0.667767    0.205063    Biso    1.000000 N
    N19     1.0     0.205568    0.667769    0.205047    Biso    1.000000 N
    N20     1.0     0.794426    0.332224    0.205069    Biso    1.000000 N
    N21     1.0     0.462158    0.794390    0.205309    Biso    1.000000 N
    N22     1.0     0.537840    0.205602    0.205291    Biso    1.000000 N
```

N23	1.0	0.332213	0.537856	0.204936	Biso	1.000000 N
N24	1.0	0.667777	0.462158	0.204926	Biso	1.000000 N
C1	1.0	0.539524	0.145678	0.203820	Biso	1.000000 C
C2	1.0	0.460484	0.854320	0.203831	Biso	1.000000 C
C3	1.0	0.854335	0.393842	0.203247	Biso	1.000000 C
C4	1.0	0.145670	0.606152	0.203213	Biso	1.000000 C
C5	1.0	0.606182	0.460493	0.203173	Biso	1.000000 C
C6	1.0	0.393804	0.539515	0.203193	Biso	1.000000 C
C7	1.0	0.145700	0.539513	0.203158	Biso	1.000000 C
C8	1.0	0.854308	0.460486	0.203166	Biso	1.000000 C
C9	1.0	0.393828	0.854324	0.203825	Biso	1.000000 C
C10	1.0	0.606185	0.145679	0.203814	Biso	1.000000 C
C11	1.0	0.460473	0.606154	0.203257	Biso	1.000000 C
C12	1.0	0.539516	0.393849	0.203251	Biso	1.000000 C
C13	1.0	0.600531	0.266900	0.207270	Biso	1.000000 C
C14	1.0	0.399470	0.733100	0.207285	Biso	1.000000 C
C15	1.0	0.733139	0.333631	0.207178	Biso	1.000000 C
C16	1.0	0.266862	0.666375	0.207172	Biso	1.000000 C
C17	1.0	0.666349	0.399463	0.207119	Biso	1.000000 C
C18	1.0	0.333649	0.600552	0.207127	Biso	1.000000 C
C19	1.0	0.266894	0.600553	0.207118	Biso	1.000000 C
C20	1.0	0.733112	0.399461	0.207119	Biso	1.000000 C
C21	1.0	0.333615	0.733103	0.207281	Biso	1.000000 C
C22	1.0	0.666385	0.266897	0.207280	Biso	1.000000 C
C23	1.0	0.399499	0.666376	0.207180	Biso	1.000000 C
C24	1.0	0.600502	0.333632	0.207164	Biso	1.000000 C
Sb1	1.0	0.500015	0.000002	0.157572	Biso	1.000000 Sb
Sb2	1.0	0.000004	0.499984	0.156462	Biso	1.000000 Sb
Sb3	1.0	0.499993	0.500004	0.156501	Biso	1.000000 Sb

```
#======================================================================
# CRYSTAL DATA
#----------------------------------------------------------------------
data_VESTA_phase_1
_pd_phase_name                         'BiN3O1                        '
_cell_length_a                         21.89000
_cell_length_b                         21.89000
_cell_length_c                         20.00000
_cell_angle_alpha                      90
_cell_angle_beta                       90
_cell_angle_gamma                      120
_symmetry_space_group_name_H-M         'P 1'
_symmetry_Int_Tables_number            1
```

```
loop_
_symmetry_equiv_pos_as_xyz
   'x, y, z'

loop_
   _atom_site_label
   _atom_site_occupancy
   _atom_site_fract_x
   _atom_site_fract_y
   _atom_site_fract_z
   _atom_site_adp_type
   _atom_site_B_iso_or_equiv
   _atom_site_type_symbol
   H1    1.0    0.435446    0.342734    0.173349    Biso    1.000000 H
   H2    1.0    0.340026    0.907002    0.173801    Biso    1.000000 H
   H3    1.0    0.093853    0.434151    0.171237    Biso    1.000000 H
   H4    1.0    0.639386    0.561683    0.212993    Biso    1.000000 H
   H5    1.0    0.362585    0.441927    0.213851    Biso    1.000000 H
   H6    1.0    0.918828    0.359506    0.215449    Biso    1.000000 H
   H7    1.0    0.075903    0.636373    0.210042    Biso    1.000000 H
   H8    1.0    0.439329    0.078471    0.213322    Biso    1.000000 H
   H9    1.0    0.558855    0.921406    0.212558    Biso    1.000000 H
   N1    1.0    0.486177    0.079489    0.207691    Biso    1.000000 N
   N2    1.0    0.511905    0.920809    0.209332    Biso    1.000000 N
   N3    1.0    0.919410    0.406367    0.211046    Biso    1.000000 N
   N4    1.0    0.077881    0.590853    0.206397    Biso    1.000000 N
   N5    1.0    0.593228    0.514650    0.209515    Biso    1.000000 N
   N6    1.0    0.408750    0.488704    0.209153    Biso    1.000000 N
   N7    1.0    0.087801    0.476806    0.180228    Biso    1.000000 N
   N8    1.0    0.388672    0.912875    0.182873    Biso    1.000000 N
   N9    1.0    0.478279    0.391383    0.182266    Biso    1.000000 N
   N10   1.0    0.671824    0.208747    0.199050    Biso    1.000000 N
   N11   1.0    0.325856    0.790422    0.201805    Biso    1.000000 N
   N12   1.0    0.792255    0.464833    0.201143    Biso    1.000000 N
   N13   1.0    0.210095    0.536886    0.200746    Biso    1.000000 N
   N14   1.0    0.537289    0.328099    0.201828    Biso    1.000000 N
   N15   1.0    0.464936    0.673893    0.200666    Biso    1.000000 N
   N16   1.0    0.202127    0.662090    0.211132    Biso    1.000000 N
   N17   1.0    0.795508    0.336950    0.211575    Biso    1.000000 N
   N18   1.0    0.458839    0.796962    0.211263    Biso    1.000000 N
   N19   1.0    0.540482    0.203827    0.211310    Biso    1.000000 N
   N20   1.0    0.338353    0.542242    0.211547    Biso    1.000000 N
   N21   1.0    0.663547    0.460744    0.212024    Biso    1.000000 N
   O1    1.0    0.912472    0.522978    0.183146    Biso    1.000000 O
```

O2	1.0	0.610632	0.088966	0.178872	Biso	1.000000 O
O3	1.0	0.524698	0.613300	0.182921	Biso	1.000000 O
C1	1.0	0.544254	0.145275	0.205825	Biso	1.000000 C
C2	1.0	0.454670	0.855545	0.207193	Biso	1.000000 C
C3	1.0	0.854769	0.399658	0.207944	Biso	1.000000 C
C4	1.0	0.144178	0.599733	0.205664	Biso	1.000000 C
C5	1.0	0.601345	0.457038	0.207436	Biso	1.000000 C
C6	1.0	0.401247	0.546490	0.206995	Biso	1.000000 C
C7	1.0	0.148287	0.535444	0.196018	Biso	1.000000 C
C8	1.0	0.852760	0.465316	0.197508	Biso	1.000000 C
C9	1.0	0.386090	0.851918	0.197567	Biso	1.000000 C
C10	1.0	0.611710	0.148009	0.194912	Biso	1.000000 C
C11	1.0	0.466172	0.614311	0.197001	Biso	1.000000 C
C12	1.0	0.536447	0.388853	0.197529	Biso	1.000000 C
C13	1.0	0.602125	0.266108	0.210714	Biso	1.000000 C
C14	1.0	0.398044	0.734427	0.210555	Biso	1.000000 C
C15	1.0	0.733805	0.336427	0.210256	Biso	1.000000 C
C16	1.0	0.265258	0.663919	0.211079	Biso	1.000000 C
C17	1.0	0.665047	0.399449	0.211271	Biso	1.000000 C
C18	1.0	0.337273	0.603286	0.210609	Biso	1.000000 C
C19	1.0	0.268578	0.600155	0.208788	Biso	1.000000 C
C20	1.0	0.732002	0.401602	0.208787	Biso	1.000000 C
C21	1.0	0.329928	0.731330	0.209223	Biso	1.000000 C
C22	1.0	0.668122	0.268268	0.207741	Biso	1.000000 C
C23	1.0	0.401191	0.669820	0.208337	Biso	1.000000 C
C24	1.0	0.600051	0.331871	0.209376	Biso	1.000000 C
Bi1	1.0	0.500190	0.001723	0.148770	Biso	1.000000 Bi
Bi2	1.0	-0.001680	0.498526	0.148936	Biso	1.000000 Bi
Bi3	1.0	0.502012	0.504002	0.149795	Biso	1.000000 Bi

References

1 J. Nørskov, J. Rossmeisl, A. Logadottir and L. Lindqvist, *J. Phys. Chem. B.,* 2004, **108**, 17886-17892.

2 A. Valdes, Z. Qu and G. Kroes, *J. Phys. Chem. C*., 2008, **112**, 9872-9879.

3 P. Atkins and J. Paula, Oxford University Press, 2014.

4 H. Hansen, V. Viswanathan and J. Nørskov, *J. Phys. Chem. C.,* 2014, **118**, 6706-6718.

5 V. Tripkovic, E. Skulason, S. Siahrostami, J. Nørskov and J. Rossmeisl, *Electrochim. Acta.*, 2010, **55**, 7975-7981.

6 J. Zhang, Z. Zhou, F. Wang, Y. Li and Y. Jing, *ACS Sustainable Chem*. *Eng*., 2020, **8**, 7472-7479.

7 R. Ouyang, E. Ahmetcik, C. Carbogno, M. Scheffler and L. Ghiringhelli, *J. Phys.: Mater.,* 2019, **2**, 024002.

8 R. Ouyang, S. Curtarolo, E. Ahmetcik, M. Scheffler and L. Ghiringhelli, *Phys. Rev. Mater.,* 2018, **2**, 083802.

9 G. Kresse and J. Furthmuller, *Comput. Mater. Sci*., 1996, **6**, 15-50.

10 G. Kresse and J. Furthmuller, *Phys. Rev. B: Condens. Matter Mater. Phys*., 1996, **54**, 11169-11186.

11 P. Blöchl, *Phys. Rev. B: Condens. Matter Mater. Phys*., 1994, **50**, 17953-17979.

12 J. Perdew, M. Ernzerhof and K. Burke, *J. Chem. Phys*., 1996, **105**, 9982-9985.

13 J. Perdew, K. Burke and M. Ernzerhof, *Phys. Rev. Lett*., 1996, **77**, 3865-3868.

14 S. Grimme, J. Antony, S. Ehrlich and H. Krieg, *J. Chem. Phys*., 2010, **132**, 154104-154123.

15 H. Monkhorst and J. Pack, *Phys. Rev. B: Condens. Matter Mater. Phys*., 1976, **13**, 5188-5192.

16 K. Mathew, R. Sundararaman, K. Letchworth-Weaver, T. Arias and R. Hennig, *J. Chem. Phys*., 2014, **140**, 084106-084114.

17 J. Glenn, M. Martyna and M. Tuckerman, *J. Chem. Phys*., 1992, **97**, 2635-2643.

18 W. Tang, E. Sanville and G. Henkelman, *J. Phys. Condens., Matter*., 2009, **21**, 084204.

19 Y. Zhou, L. Sheng, L. Chen, W. Zhang and J. Yang, *Chinese Chem. Lett*., 2025, **36**, 109588.